Magnetic properties of Au_{core}-Co_{shell} nanoparticles

Tianlong Wen and Kannan M. Krishnan[a)]
Department of Materials Science and Engineering, University of Washington, Box 352120, Seattle, Washington 98195-2120, USA

(Presented 18 November 2010; received 7 September 2010; accepted 5 November 2010; published online 24 March 2011)

Au_{core}-Co_{shell} nanoparticles were synthesized by a wet-chemical method, and their magnetic properties were characterized. By comparing the blocking temperature of Au_{core}-Co_{shell} nanoparticles to pure cobalt nanoparticles of the same size, it is proposed that cobalt spins in the shell are all aligned by exchange interaction to form single domain nano shells. At the same time, a demagnetizing field in the gold core develops and is aligned along the magnetization direction of the cobalt shell. A greatly enhanced coercivity of Au_{core}-Co_{shell} nanoparticles at 10 K, compared to the pure cobalt sample, was observed. We propose that the enhanced coercivity of Au_{core}-Co_{shell} nanoparticles is due to the pinning effect of cobalt spins at the Au/Co interface. The pinning mechanisms include strain pinning and demagnetizing field pinning. © *2011 American Institute of Physics*. [doi:10.1063/1.3544493]

Recently, core-shell nanoparticles (NPs) with magnetic components have attracted much interest in both fundamental research[1] and practical applications.[2] In magnetic core-shell NPs, the novel properties of magnetic components can be combined with those of another active component to make bifunctional or even multifunctional NPs.[3] However, many fundamental but critical properties of these magnetic core-shell NPs are still not well understood. The blocking temperature (T_B) of NPs with a magnetic core and a nonmagnetic shell is mainly determined by the size of the magnetic core.[4] The slightly reduced T_B in ensembles of core-shells, compared to pure magnetic NPs of the same size as the magnetic core, is attributed to the increased spacing (decreased interaction) between magnetic cores.[5] However, magnetic properties of the inverse structure, namely, NPs with a nonmagnetic core and a magnetic shell, have rarely been studied. Here, magnetic properties of Au_{core}-Co_{shell} NPs, an immiscible core-shell nanostructure fabricated by a wet chemical method, were studied to address such an inverse core-shell nanostructure. We show that the cobalt spins in the shell are all aligned in one direction to form a single domain magnetic shell with T_B approximately determined by the size of the core and shell combined. Furthermore, a greatly enhanced coercivity of core-shell NPs compared to pure cobalt NPs of the same size has been observed and is attributed to the pinning effect of cobalt spins at the Au/Co interface.

Following our earlier work on synthesis,[6] self-assembly,[7] and morphology[8] of cobalt based NPs, here we focus on Au_{core}-Co_{shell} NPs, synthesized by a seed-mediated sequential growth method in an organic solvent.[9] In this method, gold precursor NPs were synthesized, followed by heterogeneous nucleation of cobalt monomers on the surface of gold precursor NPs to yield core-shell nanostructures. Firstly, to fabricate gold precursor nanoparticles, $AuCl_4^-$ ions were transferred from aqueous phase to organic solvent to form $[N(C_8H_{17})_4]^+AuCl_4^-$ by mixing $HAuCl_4$ in de-ionized (D. I.) water with tetraoctylammonium bromide in toluene during vigorous stirring. After that, a linear amine was added to the mixture, followed by the addition of sodium borohydride ($NaBH_4$) in D. I. water to reduce gold ions to form gold NPs.[10] As-synthesized gold precursor NPs were coated with amine layers and dispersed in the toluene phase. After separation from the aqueous phase, gold nanoparticles in toluene were washed with methanol, precipitated by centrifuge, dried in vacuum, and then redispersed in toluene to make gold precursor solutions. In 10 mL of toluene, we dissolved and sonicated 0.05 g of gold nanoparticles which were then degassed carefully for 30 min by argon to expel all oxygen in the Schlenk line. The gold precursor solution was then heated up to 90 °C, at which temperature 0.1 g $Co_2(CO)_8$ in 3 mL toluene with extra oleylamine and oleic acid, prepared in a glovebox filled with pure argon gas, was slowly injected into the hot gold precursor solution. Due to a lower activation energy of heterogeneous relative to homogeneous nucleation of cobalt, decomposed cobalt monomers preferentially coat the surface of gold precursor NPs to yield Au_{core}-Co_{shell} NPs. The product was stored in a glass vial filled with argon and kept in a glovebox to prevent oxidation. As-made Au_{core}-Co_{shell} NPs were characterized using a FEI Tecnai G2 F20 microscope operated at 200 kV and a Phillips CM 100 electron microscope operated at 100 kV. The magnetic properties of as-synthesized Au_{core}-Co_{shell} as well as the cobalt (as a control sample) NP powder were also characterized by a Physical Properties Measurement System (PPMS).

A bright field transmission electron microscopy (TEM) image of as-synthesized Au_{core}-Co_{shell} NPs is shown in Fig. 1(a), with a magnified small area shown in the inset. Histograms of the size of gold cores and whole NPs are shown in Figs. 1(b) and 1(c), respectively; the histogram of the size ration (gold core to whole particle) is plotted in Fig. 1(d). On average, the physical size of a whole Au_{core}-Co_{shell} NP is ~10 nm, with a nonmagnetic gold core of ~5 nm. Due to the heterogeneous nucleation of cobalt atoms on the surface of gold seeds during synthesis, the cobalt shell is multi-grained around a single crystalline gold core, resolved by the high resolution TEM (HRTEM) and its irregular fast Fourier transformation (FFT)

a)Author to whom correspondence should be addressed. Electronic mail: kannanmk@uw.edu.

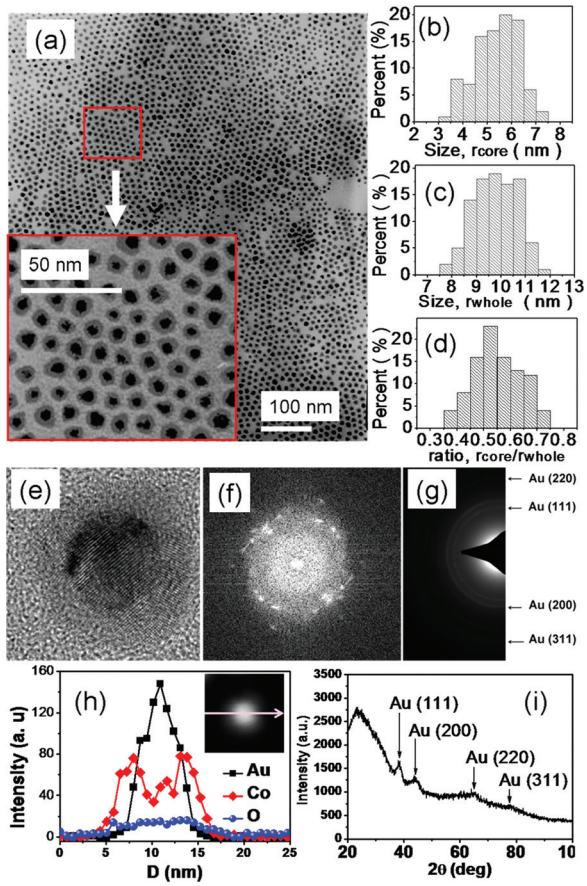

FIG. 1. (Color online) Bright field TEM (a), histogram of the size of gold core (b), histogram of the size of whole particle (c), histogram of gold core to whole particle ratio (d), HRTEM (e) and its corresponding FFT (f), SAED (g) and EDX line scan with a probe size ~ 1nm (h) and XRD θ-2θ scan (i) of Au_{core}-Co_{shell} nanoparticles. The inset in (h) shows the STEM image of the particle and the direction of the EDX line scan.

pattern, as shown in Figs. 1(e) and 1(f), respectively. Such chemically synthesized Au_{core}-Co_{shell} NPs are not in complete equilibrium, which might affect their magnetic properties. To achieve their equilibrium configuration, additional energy at the grain boundary in the cobalt shell, Au/Co interface, and strain in both gold core and cobalt shell,[11] has to be minimized. Electron diffraction rings of as-synthesized Au_{core}-Co_{shell} NPs in Fig. 1(g) can only be indexed as the face centered cubic gold crystals, which is consistent with x-ray θ–2θ scans with Cu $K\alpha$ radiation, shown in Fig. 1 (i). The absence of diffraction rings of cobalt crystal is due to the small size of cobalt crystallites in the shell as a result of heterogeneous nucleation of cobalt atoms on the surface of gold NPs. Fig. 1(h) shows the energy-dispersive x-ray spectroscopy (EDX) line scan across a Au_{core}-Co_{shell} NP in scanning TEM (STEM) mode with an electron probe of a diameter ~1 nm. The line profiles of gold and cobalt in Fig. 1(h) indicate that gold is located at the center surrounded by cobalt, clearly confirming the formation of the Au_{core}-Co_{shell} morphologies. The very small oxygen signal around the whole particle is attributed to the carboxylic group (—COOH) coating of oleic acid on the outermost surface of the cobalt shell,[12] and/or a minute oxidation at the surface of the cobalt shell.

Due to the multi-grained nature of the cobalt shell in the Au_{core}-Co_{shell} NPs, cobalt spins in the shell may have two possible configurations. As shown in Fig. 2(c) spins in each cobalt grain may be spontaneously aligned along one direction by exchange interaction, but different cobalt grains behave independently, and spins in different cobalt grains are configured to minimize magnetostatic and magnetocrystalline energy. In this configuration, exchange energy at the interface between cobalt crystallites, due to a small angle mismatch between the magnetization directions of adjacent cobalt crystallites, are compensated by the minimization of magnetostatic energy and magnetocrystalline energy. Alternatively, cobalt spins in the shell are all aligned along one direction by exchange interactions, as shown in Fig. 2(d). The T_B of as-synthesized Au_{core}-Co_{shell} NPs is ~225 K, as determined by the temperature associated with the maximum magnetic moment of the sample in the zero field cooling (ZFC) measurement in Fig. 2(a). As a control sample, ZFC and field cooling (FC) measurements were also performed on pure cobalt NPs with a physical size [~10 nm, determined by the bright field TEM images, Fig. 2(b)] comparable in size to the whole Au_{core}-Co_{shell} NPs. The T_B of ~10 nm pure cobalt NPs, determined from the ZFC curve in Fig. 2(b), is also ~225 K, which is consistent with previous observation in our group.[13] Namely, the T_B of Au_{core}-Co_{shell} NPs is dependent on the size of the whole core-shell NPs rather than on the size of the individual cobalt grains (grain size < 4 nm with $T_B < 50$ K[13]) in contrast to the control sample of cobalt NPs.

The observation above shows that cobalt spins in the shell are all aligned along a single direction by exchange interactions, and they will rotate coherently when subjected to an external magnetic field, as shown in Fig. 2(d). In fact, for a single domain magnetic NP, its T_B is dependent on its volume, namely, $K_{eff}V = 25k_BT_B$, for a 100 second measurement window.[14] Here K_{eff}, V, and k_B are the effective magnetic anisotropy, volume of ferromagnetic component in a particle, and Boltzmann's constant, respectively; we assume gold contact with cobalt does not affect K_{eff} due to the immiscibility of gold and cobalt.[4] In other words, the T_B is proportional to the volume of the ferromagnetic component in a particle. For a typical Au_{core}-Co_{shell} NP with core size ~5 nm and whole size ~10 nm, the volume ratio of gold core to whole particle is $\sim(5/10)^3 = 1/8$. Hence, even though their size is comparable ($radius_{Au}$: $thickness_{Co}$~1:1), the volume of the gold core is only a small portion of the volume of the whole Au_{core}-Co_{shell} NP. As a result, Au_{core}-Co_{shell} NPs behave similarly to cobalt NPs of the same size. Furthermore, in these single domain Au_{core}-Co_{shell} NPs, due to an accumulation of magnetostatic charges at the Au/Co interface [Fig. 2(d)], a demagnetizing field in the gold core is developed along the magnetization direction of the cobalt shell. This demagnetizing field in the nonmagnetic inclusion has the same direction as the magnetization direction of the cobalt shell. When the magnetization direction of the cobalt shell rotates due to thermal fluctuation and/or an external magnetic field, rotation of this demagnetizing field will be aligned along the magnetization direction of the cobalt shell.

Magnetic hysteresis loops at different temperatures of Au_{core}-Co_{shell} NPs were measured using the VSM mode of our PPMS system and compared with the control sample of cobalt NPs. Figure 3 shows the magnetic hysteresis loops of cobalt

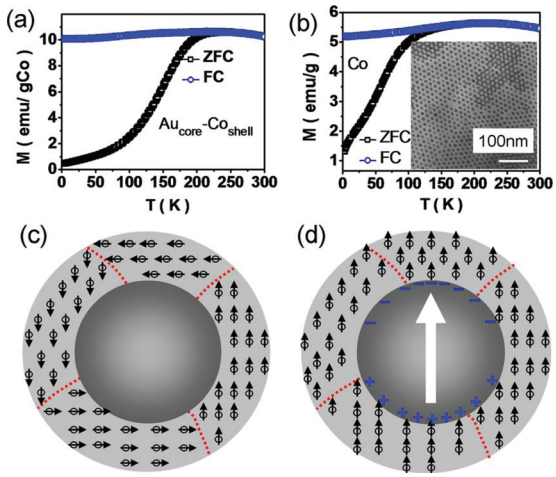

FIG. 2. (Color online) The ZFC/FC curve of (a) Au_{core}-Co_{shell} and (b) cobalt nanoparticles. The blocking temperatures (T_B) of the two samples are the same, ~225 K, and the inset in (b) shows the bright field TEM image of pure cobalt nanoparticles. The two possible spin configurations of the multi-grained Au_{core}-Co_{shell} nanoparticles: (c) multiple domains and (d) a single domain, where the dotted lines represent grain boundaries. Magnetostatic charges and the demagnetizing field (arrow) in the single domain configuration are also shown in (d).

Fig. 3(a) and Au_{core}-Co_{shell} NPs Fig. 3(b) at 10 K. At this temperature ($<T_B$), both Au_{core}-Co_{shell} and cobalt NPs are ferromagnetic, leading to open magnetic hysteresis loops. Coercivity (H_C) of cobalt NP powders at 10 K is ~380 Oe [Fig. 3(a)], which is consistent with previous observations of ~9–10 nm pure cobalt NPs.[6,15] Conversely, even though their T_B is approximately the same (~225 K), the coercivity of Au_{core}-Co_{shell} NPs (H_C~3300 Oe) is much larger than that of cobalt NPs, as shown in Fig. 3. Furthermore, even though minute oxygen oxidation has been observed around whole particles in the EDX line scan in Fig. 1(h), no obvious shift due to exchange bias[16–18] has been observed in both hysteresis loops of pure cobalt and Au_{core}-Co_{shell} NPs. In fact, exchange bias coupling between the ferromagnetic cobalt and antiferromagnetic cobalt oxide (CoO) at the outermost surface will quickly be reduced as the thickness of CoO decreases.[19] As a result, Au_{core}-Co_{shell} NPs with a very thin CoO layer are often accompanied with no enhanced coercivity due to exchange bias effect.[19] Thus, the greatly enhanced H_C of Au_{core}-Co_{shell} NPs cannot be attributed to the indiscernible CoO layer at the outermost cobalt surface. Here, we propose two alternative mechanisms based on cobalt spins at the Au/Co interface being pinned to enhance the coercivity of Au_{core}-Co_{shell} NPs. First, cobalt spins at the Au/Co interface can be pinned by the strain due to the lattice mismatch of gold and cobalt. The Au/Co interface in the as-synthesized Au_{core}-Co_{shell} NPs has a great deal of disorder due to multiple nucleation sites during heterogeneous nucleation,[11] and is often associated with large strain with energy given by $E_S = 2\mu V\epsilon^2(1+\sigma)/9(1-\sigma)$, where μ, ϵ, σ and V are the shear modulus, strain, Poisson's ratio, and volume of core, respectively.[20] Such an interface strain in the single domain magnetic NPs can pin the spin rotation at the interface, and thus enhance the coercivity of magnetic NPs.[21,22] Second, when switching the magnetization direction of cobalt shells, magnetostatic charges will be distributed at the Au/Co interface. To rotate the demagnetizing field along with the magnetization is analogous to exerting a pinning

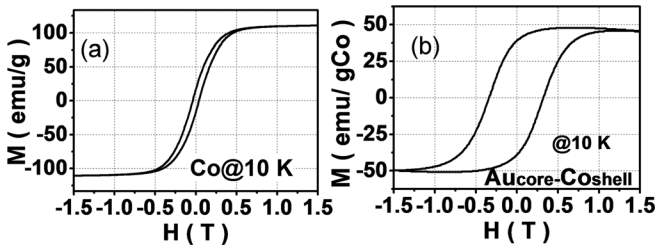

FIG. 3. Magnetic hysteresis loops of cobalt (a) and Au_{core}-Co_{shell} (b) nanoparticles at 10 K.

effect on the cobalt spins at the rough Au/Co interface. Furthermore, in this research, we found that the T_B of single domain Au_{core}-Co_{shell} NPs are mainly determined by their ferromagnetic volume but rarely determined by the Au/Co interface anisotropy (or interface pinning). However, its coercivity is greatly enhanced by the interface pinning effect. This result is consistent with previous studies.[23] However, further work is needed to understand the interplay between bulk anisotropy and interface/surface anisotropy and how they relate to T_B and H_C of single domain magnetic NPs.

In conclusion, cobalt spins in the chemically synthesized Au_{core}-Co_{shell} NP are all aligned along a single direction by exchange interaction to form single domain magnetic nanoshells. Demagnetizing fields in the gold core are developed and aligned along the magnetization direction of cobalt shells. Due to the pinning effect of cobalt spins at the Au/Co interface a greatly enhanced coercivity of Au_{core}-Co_{shell} NPs, compared to pure cobalt NPs of the same size, was observed. This technique is of possible interest to enhance the coercivity of single domain magnetic NPs.

This project is partially supported by the National Science Foundation Grant No. DMR 0501421 and the Murdock Foundation. Part of this work was conducted at the UW-NTUF, a member of NSF-NNIN.

[1]H. Zeng *et al.*, Appl. Phys. Lett. **85**, 792–794 (2004).
[2]V. Salgueirino-Maceira and M. A. Correa-Duarte, Adv. Mater. **19**, 4131 (2007).
[3]H. Kim *et al.*, J. Am. Chem. Soc. **127**, 544 (2005).
[4]Y. Bao, H. Calderon, and K.M. Krishnan, J. Phys. Chem. C. **111**, 1941 (2007).
[5]J. Wang *et al.*, J. Phys. Chem. B **109**, 21593 (2005).
[6]V. F. Puntes, K. M. Krishnan, and P. A. Alivisatos, Top. Catal. **19**, 145 (2002).
[7]Y. Bao, M. Beerman, and K. M. Krishnan, J. Magn. Magn. Mater. **266**, L245 (2003).
[8]Y. Bao, M. Beerman, A. B. Pakhomov, and K. M. Krishnan, J. Phys. Chem. B **109**, 7220 (2005).
[9]W. Shi *et al.*, Nano Lett. **6**, 875 (2006).
[10]M. Brust *et al.*, J. Chem. Soc. Chem. Commun. 801 (1994)
[11]T. Wen and K. M. Krishnan, J. Phys. Chem. C **114**, 14838 (2010).
[12]N. Wu *et al.*, Nano Lett. **4**, 383–386 (2004).
[13]Y. Bao and K. M. Krishnan, J. Magn. Magn. Mater. **293**, 15 (2005).
[14]D. L. Leslie-Pelecky and R. D. Rieke, Chem. Mater. **8**, 1770 (1996).
[15]S. Sun and C. B. Murray, J. Appl. Phys. **85**, 4325 (1999).
[16]J. Nogués and I. K. Schuller, J. Magn. Magn. Mater. **192**, 203 (1999).
[17]A. E. Berkowitz and K. Takano, J. Magn. Magn. Mater. **200**, 552 (1999).
[18]V. Skumryev *et al.*, Nature **423**, 850 (2003).
[19]M. Feygenson *et al.*, Phys. Rev. B **81**, 195445 (2010).
[20]J. D. Eshelby, Proc. R. Soc. London, Ser. A **241**, 376 (1957); **252**, 561 (1959).
[21]Y. C. Wang *et al.*, Appl. Phys. Lett. **84**, 2596 (2004).
[22]B. H. Liu and J. Ding, Appl. Phys. Lett. **88**, 042506 (2006).
[23]Q. Song and J. Z. Zhang, J. Am. Chem. Soc. **126**, 6164 (2004).